Brain Structure and Function (2021) 226:2375–2386
https://doi.org/10.1007/s00429-021-02337-1

ORIGINAL ARTICLE

Anatomy and histology of the Göttingen minipig adenohypophysis with special emphasis on the polypeptide hormones: GH, PRL, and ACTH

Laura Tvilling[1] · Mark West[1] · Andreas N. Glud[1] · Hamed Zaer[1] · Jens Christian H. Sørensen[1] · Carsten Reidies Bjarkam[2] · Dariusz Orlowski[1]

Received: 18 December 2020 / Accepted: 1 July 2021 / Published online: 7 July 2021

Abstract

The pituitary is involved in the regulation of endocrine homeostasis. Therefore, animal models of pituitary disease based on a thorough knowledge of pituitary anatomy are of great importance. Accordingly, we aimed to perform a qualitative and quantitative description of polypeptide hormone secreting cellular components of the Göttingen minipig adenohypophysis using immunohistochemistry and stereology. Estimates of the total number of cells immune-stained for adrenocorticotrophic hormone (ACTH), prolactin (PRL), and growth hormone (GH) were obtained with the optical fractionator technique using Stereo Investigator software. Moreover, 3D reconstructions of cell distribution were made. We estimated that the normal minipig adenohypophysis contains, on average, 5.6 million GH, 3.5 million PRL, and 2.4 million ACTH producing cells. The ACTH producing cells were widely distributed, while the PRL and GH producing cells were located in clusters in the central and lateral regions of the adenohypophysis. The morphology of the hormone producing cells also differs. We visualized a clear difference in the numerical density of hormone producing cells throughout the adenohypophysis. The relative proportions of the cells analyzed in our experiment are comparable to those observed in humans, primates, and rodents; however, the distribution of cells differs among species. The distribution of GH cells in the minipig is similar to that in humans, while the PRL and ACTH cell distributions differ. The volume of the pituitary is slightly smaller than that of humans. These data provide a framework for future large animal experimentation on pituitary function in health and disease.

Keywords Adenohypophysis · Growth hormone · Adrenocorticotropic hormone · Prolactin · Göttingen minipig · Stereology

Introduction

The adenohypophysis maintains body homeostasis through the production and feedback regulation of trophic hormones (Bargmann 1949; Bargmann et al. 1950; Catt 1970; Harris 1948; Hong et al. 2016; Koeppen et al. 2018). Disturbances in this part of the pituitary gland are commonly associated with pituitary adenomas, ischemia, or iatrogenic radiotherapy (Arafah 1986; Arafah et al. 1994; Cushing 1912; Heidelbaugh 2016; Molitch 2017). Changes in the adenohypophysis can be observed in other diseases and their models, such as models of Duchenne muscular dystrophy (de Lima 2007; Hofmann 2020). Recently, it has been shown that hormone producing cells of the pituitary can regenerate. This has opened up a new line of research with stem cells and cell transplantation regenerative therapies (Glud et al. 2016; Ozone 2016; Willems et al. 2016).

The Center for Experimental Neuroscience (CENSE) has been developing translational pig models of the nervous system disorders for the past 20 years using Göttingen minipigs (GM) (Bjarkam et al. 2004; Christensen et al. 2018; Glud et al. 2011; Jensen et al. 2009; Lillethorup et al. 2018; Norgaard Glud et al. 2010; Orstrup et al. 2019; Rosendal et al. 2010). The GM has a large gyrencephalic brain and maintains a constant body weight when kept on a strict diet. This

✉ Dariusz Orlowski
Dariusz.orlowski@gmail.com

[1] CENSE, Department of Neurosurgery and the Department of Clinical Medicine, Aarhus University Hospital, Aarhus University, 8200 Aarhus N, Denmark

[2] Department of Neurosurgery and the Department of Clinical Medicine, Aalborg University Hospital, 9100 Aalborg, Denmark

facilitates the use of magnetic resonance imaging (MRI) and stereotaxic brain surgery with devices used on humans. Compared to non-human primates, the GM is preferable with regard to ethical and economic considerations. These characteristics make the GM ideal for large animal models of CNS disease (Bjarkam et al. 2004, 2017b; Christensen et al. 2018; Goodman and Check 2002; Lillethorup et al. 2018; Lind et al. 2007; Orstrup et al. 2019; Sauleau et al. 2009). Atlases of the minipig brain are available (Bjarkam et al. 2016; Orlowski et al. 2019; Watanabe et al. 2001) and although the porcine pituitary has been described before, it were either qualitative descriptions of the hormone producing cells (Dacheux 1980, 1981, 1984) or semi-quantitative descriptions of GH producing cells (Lee 2006; Lee et al. 2004). To our knowledge, this is the first detailed study of the polypeptide hormone producing cells of the Göttingen minipig.

Our group is developing a minipig model of growth hormone deficiency by partially ablating the pituitary (Orstrup et al. 2019), which created the need for a detailed, quantitative, and qualitative description of the cytoarchitectonic and cytochemical composition of the minipig adenohypophysis.

The present study focuses on cells that produce growth hormone (GH), and, in addition, other polypeptide hormones: prolactin (PRL), and adrenocorticotrophic hormone (ACTH), because these are the most abundant cells in the adenohypophysis (Amar and Weiss 2003).

Methods

Animals and tissue processing

The study included five female GM aged 8–11 months, with a weight of 18–26 kg. The GM has to be at least 7 months of age to ensure sexual maturity (Peter et al. 2016). Measurements of the pituitary size were done using caliper on the freshly explanted glands (before fixation) removed in autopsies during our other experiments (nine female and six male GM, aged 6 months). All procedures were conducted in accordance with rules from the Danish National Council of Animal Research Ethics and with permission from the Danish Animal Inspectorate (no. 2016-15-0201-00935).

The animals were anesthetized with an intramuscular injection of midazolam (0.8 mg/kg) and S-ketamine (20 mg/kg) and euthanized with a lethal intracardial dose of pentobarbital (Exagon vet. 400 mg/ml inj., Salfarm Denmark A/S, no.: 182831) before transcardial perfusion with 10% formalin (pH 7.4) (Ettrup, 2011). After perfusion, the brain was removed to expose and collect the pituitary from the pituitary fossa by blunt dissection (Bjarkam et al. 2017b). After surgical removal, the pituitary was immersion fixed in 10% formalin (pH 7.4) for 1 day and then transferred to 30% (w/v) sucrose solution in 0.15 M Sorensen's phosphate buffer for 1 day. Tissue was frozen for 15 s in isopentane cooled with dry ice at − 40 °C and subsequently stored at − 20 °C prior to cryosectioning. The tissue was mounted in the OCT compound and the specimen was kept frozen during sectioning (knife temperature of − 20 °C and block holder temperature of − 12 °C). The tissue was exhaustively sectioned into 50 µm thick horizontal sections which were collected as ten series spaced ten sections apart (Gundersen and Jensen 1987). The sections were then stored free-floating in DeOlmos solution at − 20 °C until immunohistochemical (IHC) staining.

During cryosectioning of two of the pituitaries, a portion of tissue was lost during fixation of the tissue to the tissue holder. The portion was estimated to be approximately 500 µm. To compensate for this, one section was assumed to be missing from each of the ten section series. To generate the most accurate stereological estimate for total number, we made an estimate of the data that would have been present in the missing section: This was accomplished using the average of the stereological data from the section just prior to and after the missing section.

Histology

The IHC staining protocols were developed individually for each primary antibody. During this thorough pilot testing, we established the optimal dilutions for antibodies and different staining detection protocols to ensure complete section penetrance and clear distinction of the cytoplasm of the hormone producing cells. Staining procedures included negative controls in which the primary antibody from the IHC protocols was omitted, and in which the staining of the hormone producing cells was absent, as well as series of dilutions of the primary antibodies from very low to very high, to find their optimal concentration. In addition, one series of the section was stained with hematoxylin and eosin (H&E) for orientation purposes.

The staining protocol for ACTH

ACTH producing cells were stained using the Avidin–Biotin complex method (ABC). Accordingly, free-floating sections from one series were initially rinsed twice in Tris-buffered saline (TBS; 0.05M; pH 7.4) for 10 min. and then once in TBS plus 1% Triton X-100 (TBS-T) for 10 min. The endogenous peroxidase was blocked by washing sections in TBS containing 3% H_2O_2 and 10% methanol two times for 15 min. following by rinsing in TBS-T for 3 × 5 min. Preincubation with TBS-T and 0.2% milk (Bidinger, Aarhus, Denmark) was performed for 30 min. prior to incubation with the primary antibody (polyclonal rabbit anti-ACTH, Merck AB902, diluted 1:32.000 in the TBS-T and 0.2%

milk solution) for 72 h at 4 °C. Hereafter, the sections were rinsed for 3 × 10 min. in TBS-T both before and next after the incubation with the secondary antibody (polyclonal goat, anti-rabbit, Biotin-labeled, Dako E0432, diluted to 1:200 in TBS-T) for 1 h at room temperature. The ABC vectastain Kit was used to incubate the sections for 1 h at room temperature with avidin-peroxidase (solution prepared 1 h before use). Sections were first rinsed in TBS-T for 2 × 10 min. and followed by a rinse in TBS for 10 min. The avidin–biotin-peroxidase complexes were visualized by exposing the sections to a 20 mM phosphate-buffered solution containing 0.1% diaminobenzidine (DAB) for 7 min. and then the same solution with 0.3% H_2O_2 for 8 min.

The staining protocol for PRL and GH

IHC for GH and PRL producing cells was performed using an indirect immune-enzyme method with an HRP (horseradish peroxidase)-labeled secondary antibody. Accordingly, free-floating sections from one series were initially rinsed 3 × 10 min. in TBS-T. The endogenous peroxidase was blocked as described above, followed by rinsing the sections in TBS for 10 min., followed by a double rinse in TBS-T for 10 min. After preincubation, the sections were incubated with the primary antibody (polyclonal rabbit anti-GH, Merck AB940 or polyclonal rabbit anti-PRL, Merck AB960, 1:4000, diluted in TBS-T and 0.2% milk solution), rinsed, and then incubated with the secondary antibody (polyclonal goat, anti-rabbit, HRP-labeled, Dako P0448, diluted to 1:400 in TBS-T) as described for ACTH. The HRP activity was visualized by exposing the sections to a 20 mM phosphate-buffered solution containing 0.1% diaminobenzidine (DAB) for 7 min. and then the same solution with 0.3% H_2O_2 for 8 min. The PRL protocol included subsequent counterstaining with PAS (periodic acid–Schiff).

After the completion of the staining protocols, the sections were rinsed in distilled H_2O three times for 1 min. and then dehydrated in alcohol and xylene, mounted with Depex, and coverslipped.

The processed sections were analyzed and digitally photographed using a Leica DM5000B microscope with an attached Leica DFC480 camera. The microphotograph (Fig. 1c) was merged of several overlapping photos in Adobe Photoshop (Adobe Inc.).

Stereology

Estimation of the total number of polypeptide hormone producing cells in the adenohypophysis of each animal was performed using the optical fractionator method (Gundersen 1986; West et al. 1991), using a Zeiss AxioPlan microscope interfaced with MBF Stereo Investigator software (MBF Bioscience). The pituitary is easily separated from the rest of the brain due to its position in the pituitary fossa. Moreover, the adenohypophysis is distinguishable from the neurohypophysis and the intermedial lobe due to its different histological nature (see "Results"). Due to the small size of the most superior part of the adenohypophysis, in humans referred to as *pars tuberalis*, and lack of a clear anatomical distinction of this structure, this part was analyzed together with other sections.The size and number of the 3D probes (disectors) were defined empirically to yield approximately 200 counts of each type of hormone producing cell (West 2012) after systematically scanning one of the section series. This number of counts has been demonstrated to provide an optimal amount of precision in the estimates of the total number (Gundersen and Jensen 1987). In this study, interactions between probes and cells were based on the appearance of cytoplasm in which the reaction product was compact. Disector counting resulted in counts at the top of the reaction product in the cell. This approach results in number-weighted unbiased estimates of the total number (Sterio 1984).

Estimates of the total number of hormone producing cells N were obtained with the optical fractionator technique (West 2012; West et al. 1991). Accordingly, the number of cells of a specific type Q^- was directly counted in a defined fraction of the volume of each adenohypophysis. This fraction was calculated as the fraction of the section thickness sampled with optical disectors (thickness sampling fraction tsf), under a known fraction of the area of the sections sampled (area sampling fraction asf), on a known fraction of the set of sections that contained the entire adenohypophysis (section sampling fraction ssf).

The estimates of the total number of cells of a particular type N for each individual were obtained with the following equation:

$$N = \sum Q^- \times \frac{1}{\text{ssf}} \times \frac{1}{\text{asf}} \times \frac{1}{\text{tsf}}.$$

The tsf was calculated as the ratio of the height of the optical disector h to the section thickness t. The asf was calculated from the ratio of the area of the disector probes A_{frame} to the area of the section between the disector probes when moving from one sample sight to the next A_{step}. The ssf is the section interval (West 2012). The stereological sampling scheme for each hormone is summarized in Table 1.

The stereological estimation procedure was carried out with unbiased systematic random sampling at all levels of the sampling scheme (i.e. section selection, placement of the sample sight, the nature of the interaction between probe and structural feature).

The series, consisting of every tenth section, a ssf of 10, throughout the entire adenohypophysis of each animal, was examined using the following sampling scheme: the height of the disector was 8 µm; A_{step} was 1100 × 1100 µm; A_{frame}

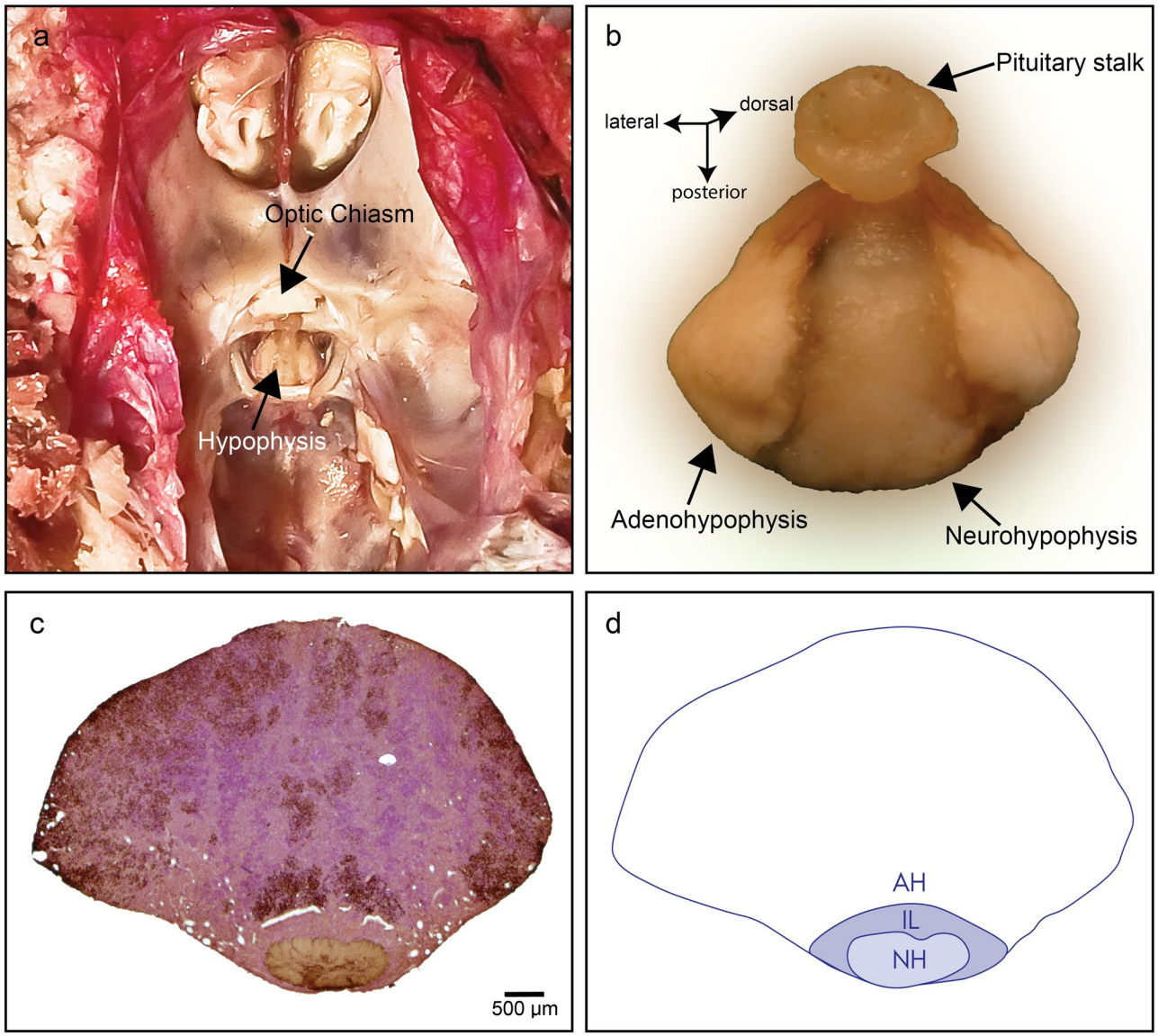

Fig. 1 **a** The minipig skull base after brain removal. Note the position of the pituitary in the pituitary fossa, **b** photography of the explanted hypophysis viewed from the posterior surface, **c** microphotography of a cross-section through the middle part of the hypophysis, stained with antibody against PRL and counterstained with PAS, **d** schematic diagram showing the anatomy of the hypophysis, as shown in **c**. *AH* adenohypophysis, *IL* intermediate lobe, *NH* neurohypophysis

Table 1 Stereological sampling scheme for individual pituitary hormone producing cells

	Abbreviations	ACTH	GH	PRL
Height of disector (µm)	H	8	8	8
Counting frame area (µm^2)	A_{frame}	2025	900	2025
Grid area $X \times Y$ (µm^2)	A_{step}	1,210,000	1,210,000	1,210,000
Disector volume ($h \times A_{\text{frame}}$)	µm^3	16,200	7200	16,200
Thickness of mounted section (µm)	T	18.3	18.0	18.9
Section sampling fraction	ssf	10	10	10
Fraction of area of section samples	asf	598	1344	598
Thickness sampling fraction	tsf	2.28	2.25	2.36
Average number of sections used	I	10	10	10

was 30 × 30 µm for GH and 45 × 45 µm for PRL and ACTH. The measured average thickness of mounted sections was 18.4 µm (18.3 for ACTH; 18.0 for GH; 18.9 for PRL).

The volume of the adenohypophysis was estimated based on Cavalieri's principle (Gundersen, 1988; Kiki et al. 2007; West 2012) by multiplying the volume of the sampled sections by the ssf. The volume of each sampled section corresponds to section thickness t multiplied by the area of section $A_{1\rightarrow n}$.

Statistical calculations of the variability of the stereological estimation protocol were carried out to optimize the sampling scheme as proposed by West (2013).

The numerical density is calculated as the number of stereological markers within the disectors divided by the total disector volume (Gundersen 1986).

Using the 'Serial Section Manager' of the Stereo Investigator system a 3D model of the GM adenohypophysis was generated. The sections were aligned according to the outline of adjacent sections and an unbiased sample of the cells on each section was used to create a spatial map of a fraction of the cells in the section. The spatial map thus reflected the statistical density and distribution of cells on individual sections. The spatial distribution of cells on all aligned sections was displayed at appropriate relative distances to create a 3D spatial distribution of the cells in the entire adenohypophysis (Online Resources 1–4).

Results

After surgical removal of the brain, the pituitary was visible in the pituitary fossa under the *diaphragma sellae* just posterior to the optic chiasm (Bjarkam et al. 2017a; Orlowski et al. 2019) (Fig. 1a). Macroscopically, the GM pituitary could be divided into two lobes and the pituitary stalk is distinctly noticeable on the superior surface (Fig. 1b). The dimensions of the minipig pituitary were as follows: height: 6.53 ± 0.74 mm, width: 7.40 ± 0.50 mm, length: 3.84 ± 0.52 mm; its weight is 101 ± 13 mg (mean ± SD, $N = 15$, age: 6 months). We did not find statistical differences between male and female pituitary size.

Microscopic evaluation of the pituitary structure made it possible to divide it into three, histologically distinct parts, namely the neurohypophysis (pars nervosa), the intermedial lobe (pars intermedia), and the adenohypophysis (pars distalis) (Fig. 1c, d). The anteriorly located adenohypophysis folds around the posteriorly located neurohypophysis and when cryosectioned, the neurohypophysis detached from the adenohypophysis indicating that the different lobes are composed of distinctively different tissues. An intermediate lobe was distinguishable in the most superior region of the GM pituitary, between the neuro- and adenohypophysis, as a slender component of different structure than both the adeno- and neurohypophysis without any of the peptide hormone producing cells present (Fig. 1c, d). The neurohypophysis consists mainly of axonal projections, which are clearly visible when using PAS (Fig. 1c) or H&E staining.

The adenohypophysis consists of multiple endothelial cells (glandular epithelial tissue). H&E staining reveals basophils, acidophils, and chromophobes in the adenohypophysis but no distinction between different hormone producing cells or visualization of density or distribution patterns.

The use of immunohistochemical stainings of the adenohypophysis allowed us to detect specific peptide hormones in the cell cytoplasm. In all the stained sections, the cytoplasm was densely and uniformly pigmented. ACTH producing cells usually had a round or oval shape, with a relatively large nucleus located at the periphery of the cytoplasm, occasionally with only a slim rim of cytoplasm around (Fig. 2a). The shapes of GH and PRL producing cells were more polygonal and elongated with a prominent, often eccentrically situated nucleus (Fig. 2b, c, respectively).

The density and distribution patterns of hormone producing cells showed considerable intra- and intersectional differences. A more robust spatial pattern of distribution was observed when consolidating data from multiple adenohypophyses.

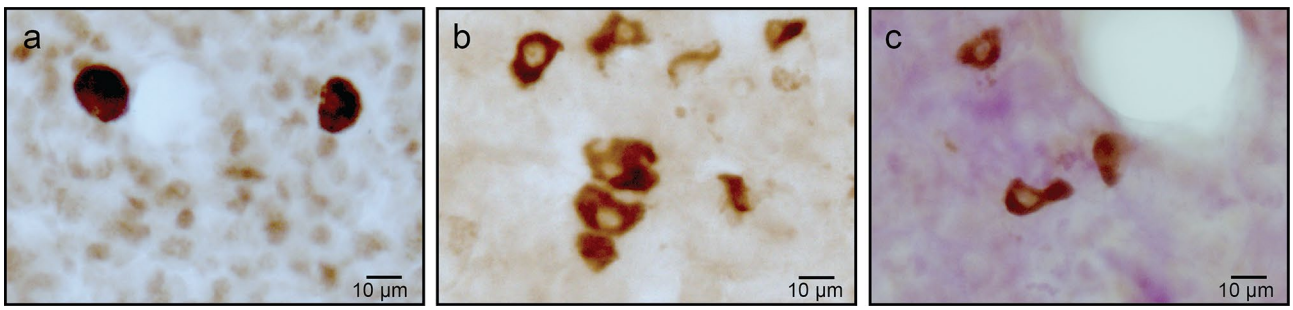

Fig. 2 Representative microphotographs of the hormone producing cells: **a** adrenocorticotropic hormone (ACTH), **b** growth hormone (GH) and **c** prolactin (PRL) counterstained with PAS

IHC staining for GH revealed a dense cluster of cells at the center of the posterior part of the adenohypophysis that borders on the neurohypophysis. However, as described below, this cluster was not as pronounced as those formed by PRL producing cells. The density of the clusters increased in the middle and inferior part of the adenohypophysis. The main feature of the distribution pattern of GH producing cells was the very densely packed regions located in the posterolateral part of the adenohypophysis. The lateral collections of cells were not visible in the most superior part of the adenohypophysis but expanded throughout the middle and inferior part of the adenohypophysis, leaving a rather large region devoid of GH producing cells in the anterior part of the adenohypophysis.

PRL producing cells were distributed in a pattern similar to that of the GH producing cells. A centrally located cell cluster in the posterior part of the adenohypophysis was present and was more distinct and dense than GH producing cells. This cluster of cells extended throughout the entire adenohypophysis from top to bottom. Furthermore, bilateral clusters of cells in the lateral part of the adenohypophysis appeared in the middle part of the adenohypophysis and continue into the inferior part. The size and density of these clusters increased progressively towards the bottom, so that only a small region in the most anterior central part of the adenohypophysis was void of PRL producing cells. The distribution pattern for ACTH producing cells differed from that of the two other peptide hormone producing cells in the adenohypophysis. There were no clearly defined cell clusters and the cells were distributed uniformly throughout the adenohypophysis.

The quantitative examination of the microscopic images revealed a clear difference in the numerical densities (number per unit volume) of the different hormone producing cells along the superior-inferior axis of the GM adenohypophysis. The differences in densities are visualized in the density graph as an average of density for all five animals (Fig. 3).

The density graph (Fig. 3) shows that the numerical density is highest for GH producing cells compared to the other peptide hormones. In addition, the numerical density of GH producing cells gradually increased along the superior–inferior axis. The ACTH producing cells had the lowest density of the three hormones examined and the density was relatively constant throughout the entire tissue. The numerical density of PRL producing cells increased progressively along the superior–inferior axis, with a small decrease in density in the most inferior region (Fig. 3).

Stereology

The GH producing cells account for approximately half of the total number of peptide hormone producing cells that were studied. The adenohypophysis of one pituitary contained on average 5.6 ($\pm 1.36 \times 10^6$) million GH producing cells compared to 2.4 ($\pm 4.99 \times 10^5$) million ACTH producing cells and 3.5 ($\pm 6.09 \times 10^5$) million PRL producing cells (Table 2). The relative proportions of different hormone producing cells are summarized in Fig. 4. The estimates

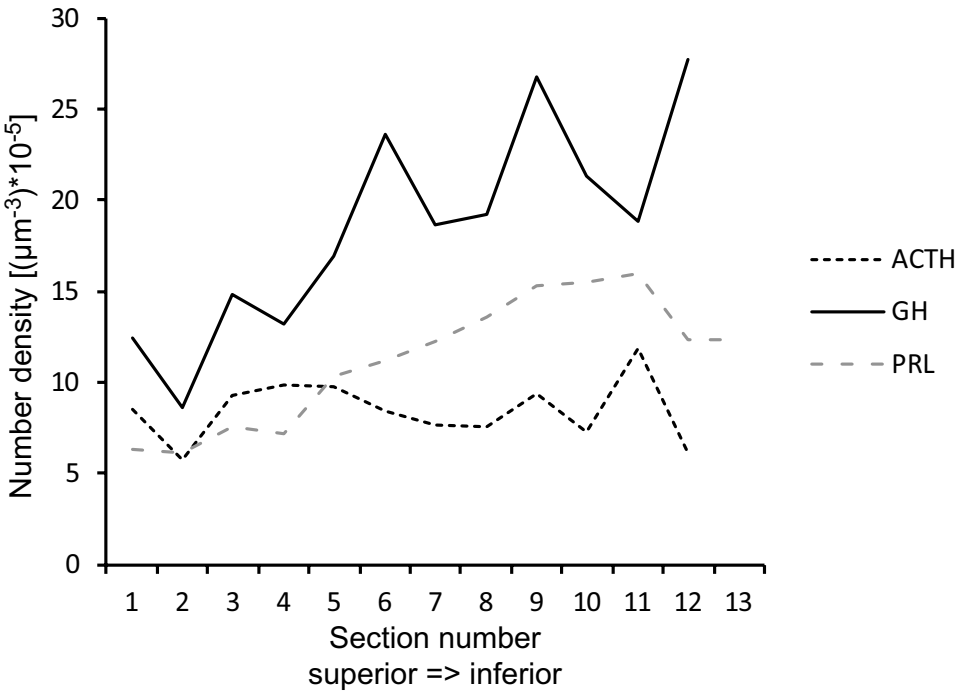

Fig. 3 Different distribution pattern of the hormone producing cells along the Göttingen minipig adenohypophysis

of the total volume of a GM adenohypophysis examined in our studies varied from 21.26 mm^3 to 35.48 mm^3 (mean 27.52 ± 4.73).

The observed relative variance of the stereological estimates was less than 20% of the observed group variance (the relative variance of the group OCV^2 is equal to the sum of the biological variance and the stereological variance). The observed relative group variance is primarily due to biological variability (Table 2).

The 3D model of the adenohypophysis provides a valuable overview of the difference in cell distribution throughout the depth of the adenohypophysis. The model is consistent with the histological data showing that ACTH producing cells were widely distributed and spread out, whereas PRL and GH producing cells formed clusters mainly in the lateral regions and a centrally located region adjacent to the neurohypophysis, which contained more PRL producing cells than GH producing cells (Online resource 1, 2, 3 and 4).

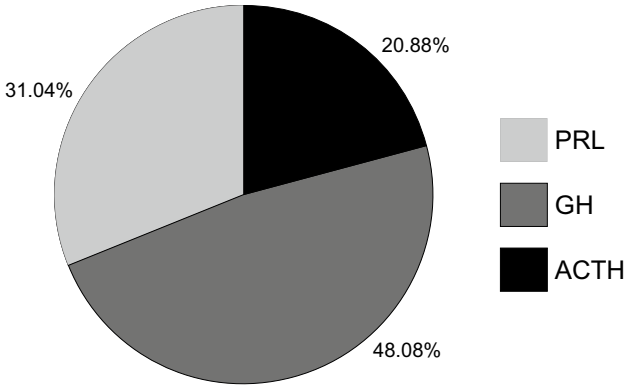

Fig. 4 Numerical composition of the main hormone producing cells in the Göttingen minipig hypophysis

Discussion

To our knowledge, this study, based on immunohistochemistry and stereological analysis, presents the first detailed quantitative anatomical description of the GM adenohypophysis and its polypeptide hormone producing cells. To perform this study, we developed a stereological protocol for estimating the total number of peptide hormone producing cells. The optical fractionator method applied in our study is an acknowledged approach for estimating cell numbers, also of the pituitary (Cruz-Orive and Weibel 1990; Deniz et al. 2018; Francis et al. 2000; Garcia-Navarro et al. 1988; Gundersen 1986; West et al. 1991). The histological and stereological analysis reveals the cellular composition of the GM pituitary and its similarity to the human pituitary (Mitrofanova et al. 2017; Musumeci, 2015). Likewise, the size of the minipig pituitary, although a bit smaller, is comparable to that of the human (approx. 10 × 12 × 5 mm) (Amar and Weiss 2003; Wolpert et al. 1984). According to Mai and Paxinos (2012), the size of the pituitary is approximately 8 × 6 × 4 mm, which is even more similar to the size observed by us in minipigs. The minipig pituitary is also approximately twice as large as that in rodents (rat: length 4 mm, width 2.2 mm, mouse: 3 × 2.2 mm) (Cao et al. 2017; Heiman 1938). Similarly to humans (Hong et al. 2016; Mai and Paxinos 2012), the GM adenohypophysis constitutes the bulk of the pituitary structure, whereas the neurohypophysis is significantly smaller and the intermediate lobe consists only of a relatively thin cell layer between adeno- and neurohypophysis (Hong et al. 2016; Mai and Paxinos 2012).

The distribution pattern of hormone producing cells in the adenohypophysis has previously been studied in multiple species (Amar and Weiss 2003; Filippa and Mohamed 2006a, b; Lee et al. 2004; Mikami et al. 1988; Naik et al. 1991; Nakane 1970; Wang, 2014) and both the density and distribution of cell types vary among species. The density and distribution analysis of this study can be useful for targeting specific regions or components of the pituitary, to achieve the optimal impact with minimal collateral damage with surgical intervention.

The GH cell distribution pattern observed in this study is highly comparable with those analyzed in prepubertal porcine pituitary (Lee et al. 2004). The prevalence of the GH producing cells in lateral parts of the adenohypophysis is also similar to human (Amar and Weiss 2003). However, the distributions of the other hormone producing cells in human are different. The ACTH producing cells are located primarily in the anteromedial part of the adenohypophysis

Table 2 Results of the stereological analysis for individual hormone producing cells

	Abbreviations	ACTH	GH	PRL
Average number of counts in each individual	$\sum Q^-$	175	183	248
Observed group mean	Mean *N*	2,394,912	5,562,774	3,511,729
Observed coefficient of variation of estimator	OCE	0.08448	0.07840	0.06937
Observed coefficient of variation of group mean	OCV	0.20832	0.24334	0.17342
Number of individuals in group	*n*	5	5	5
Biological variability	VARbiological	0.0360	0.0530	0.0252
Stereological variability	VARstereological	0.0074	0.0062	0.0049

(Amar and Weiss 2003; Trouillas et al. 1996), whilst the PRL producing cells are scattered throughout the gland. In contrast, another study of the human pituitary showed that although PRL cells are scattered throughout the adenohypophysis, they were more numerous in the posteromedial and posterolateral parts of the gland, which is comparable to our results (Asa et al. 1982). A study of the bovine pituitary reported a cell distribution similar to that of the GH and PRL producing cells, located in the lateral part of the adenohypophysis in pigs (Dacheux and Dubois 1976). In rodents, GH, PRL, and ACTH producing cells have a similar distribution pattern with the cells sparsely represented in the most anteroventral portion of the adenohypophysis, though only the PRL producing cells are represented in the region near the intermediate lobe (Nakane 1970). In more current studies of one of the rodent species (Viscacha, *Lagostomus maximus maximus*), authors reported a wide distribution of the GH producing cells in the adenohypophysis, with an exception of the cephalic extreme of the adenohypophysis, where a long blood vessel delimited a region without GH producing cells. However, in premature animals that distribution pattern was not so evident (Filippa and Mohamed 2006b). PRL producing cells were located mostly in the ventromedial region and caudal extreme of the adenohypophysis, whilst ACTH producing cells were found in the dorsal and cephalic region (Filippa and Mohamed 2006a, 2010). In the Chiroptera pituitary (Mikami et al. 1988), the GH producing cells are the most abundant cell type and located in the posterolateral part of the adenohypophysis. The PRL producing cells form a pattern similar to GH, although they are more densely packed in the central part of the adenohypophysis. The ACTH producing cells are found both in rostroventral and ventrolateral regions (Mikami et al. 1988). In contrast to these findings, the distribution pattern for hormone producing cells in the teleost differs from the mosaic pattern found in our study in that each cell type is located in separate compartments (Kasper et al. 2006). Due to this species variations, the knowledge of the distribution and density of the cell types in the minipig pituitary is of value for future studies.

The distribution patterns of PRL and GH are rather similar, except for a large, centrally located cluster of PRL producing cells, which was also noted by Lee in young pigs (Lee 2006). Therefore, qualitative microscopic observations suggest that the quantity of PRL producing cells is greater than the quantity of GH producing cells. This may also explain the higher volume densities of the PRL producing cells in some studies (Francis et al. 2000; Vanputten et al. 1988). However, the stereological data reveal that the opposite is the case. Here we show that the density of the GH producing cells in the inferior region of the adenohypophysis is particularly high compared to PRL producing cells, indicating that despite the comparable distribution pattern of clusters of GH and PRL producing cells, GH producing cells are more densely packed. This is in accordance with the findings from the bovine and the chiroptera pituitary (Mikami et al. 1988; Wang et al. 2014).

The relative proportions of the polypeptide hormone producing cells in GM, reported here, are similar to those observed in human (GH: 40–50% PRL: 10–25%, corticotrophins: 15–20%) (Amar and Weiss 2003; Mai and Paxinos 2012; Mitrofanova et al. 2017), which further supports the usability of the minipig as a model organism for pituitary polypeptide hormone deficiency. Studies of the Squirrel monkey (*Saimiri sciureus boliviensis*) showed similar cell proportions, although with a lower fraction of corticotrophs (Console et al. 2001). Interestingly, Francis et al. reported in their stereological investigation of the sheep pituitary that the relative fraction of the PRL producing cells is higher than GH producing cells (55.7% versus 37.1%) (Francis et al. 2000), which is opposite that in all above-mentioned species including pigs and humans. This, however, may be the result of a different methodology, since the authors analyzed the cell fractions using the sections taken from only three pituitary levels. However, similar results were noted in some rat studies (Vanputten et al. 1988), in which the estimated volume density of hormone producing cells was the highest in the case of PRL (PRL 40.5%, GH 22–28%, ACTH 9–11%).

It is worth mentioning that the distribution of the hormone producing cells may change with age and during the reproductive cycle (Filippa and Mohamed 2006b; Lee et al. 2004), which should be taken into consideration when comparing the results or during the planning of the experiments. Studies have shown both sexual dimorphism and age-related changes in the density of hormone producing cells in rodents (Console et al. 1997; Dada et al. 1984; Jurado et al. 1998; Sasaki and Iwama 1988). Age and sex-related differences were shown also in other species (Kuwahara et al. 2004; Tan and Sasaki 2000). There are also other factors, which can affect the hormone producing cell number and distribution, such as reproductive cycle, lactation, or time of the year (Filippa and Mohamed 2006a, 2010; Jurado et al. 1998; Nishimura et al. 2000). For example, in pony horses, the adenohypophysis has a similar cellular composition as the GM; however, there are also noted significant differences in the proportions of the hormone producing cell caused by age and sex. The relative proportion of the GH producing cells decrease with age and is higher in males, whilst PRL producing cell number increase with age and is higher in females, except old animals, where there were no differences between sexes (Kuwahara et al. 2004; Tan and Sasaki 2000). Likewise, in studies performed on mice the proportion of the GH producing cells was similar to that shown by us in GM and that cells that produced GH significantly decreased with age (Kuwahara et al. 2004). Conversely, in Viscacha, the

immune-positive region for GH increases with the age, and the highest number of somatotrophs was observed in prepubertal animals. There were also noted significant changes in the GH producing cells number in various periods of the reproductive cycle (Filippa and Mohamed 2006b). It could be that the same is true for the porcine hormones (Heiman et al. 1990; Meijer et al. 1988), which emphasizes the importance of including animals of uniform sex and age for future studies. It would be also of great value to expand our methods to male animals.

Moreover, it should be noted that according to some studies, the different pituitary hormones could be co-released from the same cells (e.g. GH/ACTH, PRL/ACTH, and GH/PRL) (Kovacs et al. 1989; Mitrofanova et al. 2017; Vidal et al. 1997). The number of such cells can be quite substantial, even more than 10% of the cells may express various combination of hormones (Mitrofanova et al. 2017). According to some studies, fraction of the cells producing both GH and PRL (somatomammotrophs) can be as high as 27% in the goat (Nishimura et al. 2000). We did not attempt to correct for such a phenomenon, which could have resulted in counting the same sub-population of the cells more than once. As a result, our estimates of the total numbers of those cells may be overstated. This problem could be solved by using double staining for different hormone combinations and counting the fraction of double-stained cells. However, the use of the light-microscope intended double staining is not recommended in stereology, due to problems with unambiguous recognition and categorization of the cell. Moreover, we did not count the cells secreting gonadotrophs and thyrotrophs, therefore the relative fraction of the cells presented here is higher than when all hormone producing cells were counted.

The number of studies in which the number of hormone producing cells has been assessed is limited. The absolute number of GH producing cells, reported by us, is approximately three times higher than observed in mice. It is also worth noting that the number of GH producing cells in mice significantly decreases with age (at 12 months 50% less than at 4 months) (Kuwahara et al. 2004). In another rat study, using stereology, the number of ACTH producing cells was around 1.4 million (Trifunovic et al. 2018), which is approximately 40% lower than the number of cells estimated by us. Trouillas et al. (1996) estimated, using semi-quantitative methods, that number of corticotropic cells in human is around 10^7, that is approx. four times more than that in the present study for GM.

We estimated the volume of the adenohypophysis using sections prepared for stereological analysis. However, estimated volumes varied both intra- and inter-individually. This is most likely the result of the naturally occurring differences in the areas between the different series of sections of a spherical structure, cut at different angles. Furthermore, we did not attempt to correct the volume for tissue shrinkage during the IHC processing, therefore the estimate of the volume is for the processed tissue (Bonthius et al. 2004; West 2013).

Observed variability of the individual estimates in the group is a result of both the stereological procedure and innate biological differences (West 2012). The coefficients of variation for estimated cell numbers were 0.069–0.084 for each hormone (Table 2) and represents an acceptable level of precision of the estimates of a total number of cells since the contribution of the stereological procedure to the observed coefficient of variation of group mean is extremely low compared to the biological variability. This fact might be used in future studies to reduce the number of analyzed sections and make the protocol less time-consuming.

The ability to divide total variance into stereological variance and biological variance is important also in the planning of future experimental studies and statistical power calculation. (West 2012). Moreover, the animals included in this study vary in regards to age. It would be preferable to perform this study on animals with the same characteristics to minimize the biological variability and hence the precision of the applied method (West 2012).

The use of the optical fractionator method for stereological estimation procedure yields unbiased, reproducible estimates of the total number of cells (West 2012; West et al. 1991). Using this method, we have shown that GM adenohypophysis is more similar to that of humans than that of the rodent. This study thereby validates the use of the GM as a good candidate for establishing a large animal model of human pituitary deficiency. The information presented here can be used to plan future experimental intervention studies involving the GM pituitary, as well as the evaluation of the effect of the intervention (Orstrup et al. 2019) or in various disease models (de Lima et al. 2007; Hofmann et al. 2020). Stereology has previously been used in experimental studies on peptide hormone producing cells in the pituitary of rats (Milosevic et al. 2009; Raus Balind et al. 2016; Trifunovic et al. 2014; Trifunovic, 2016). However, the use of large animal models provides obvious advantages compared to rodent models, in terms of both anatomy (pituitary size and macroscopic anatomy) and histology (cellular composition and distribution). A minipig model of pituitary deficiency will enable preclinical studies involving gene therapy, stem cells, and drug candidate testing. The presented quantitative, anatomical description of the minipig pituitary will strengthen the usefulness of GMs as a large animal model of pituitary disorders related to pharmacology, endocrinology, and neurosurgery.

Supplementary Information The online version contains supplementary material available at https://doi.org/10.1007/s00429-021-02337-1.

Acknowledgements This research was conducted at the Center for Experimental Neuroscience (CENSE), Department of Neurosurgery, Aarhus University Hospital. The authors sincerely thank the Department of Biomedicine, Aarhus University, for access to stereological facilities and acknowledge with gratitude the skillful assistance of Mrs. Trine W. Mikkelsen, Mrs. Lise M. Fitting, Mrs. Majken Sand, and Mrs. Anne Sofie Møller Andersen as well as the staff at Paaskehoejgaard. We would also express our gratitude to Lundbeck Foundation for funding this project.

Author contributions All authors contributed to the study conception and design, which was managed by ANG and JCS. JCS, HZ, LT, and DO collected the pituitary samples. Material preparation, histological processing, and data collection were planned and performed by LT, MW, and DO. LT, MW, CRB performed data analysis. The first draft of the manuscript was written by LT and DO, which was commented on and edited by MW, ANG, and CB. All authors read and approved the final version of the manuscript.

Funding Lundbeck Foundation and Clinical Institute, Aarhus University supported this study.

Data availability The datasets generated during and/or analyzed during the current study are available from the corresponding author on reasonable request.

Code availability Not applicable.

Declarations

Conflict of interest The authors have no relevant financial or non-financial interests to disclose.

Ethical approval All applicable international, national, and/or institutional guidelines for the care and use of animals were followed. All procedures performed in studies involving animals were approved by and in accordance with the ethical standards of the Danish National Council of Animal Research Ethics (protocol number 2016-15-0201-00935).

Consent to participate Not applicable.

Consent for publication Not applicable.

References

Amar AP, Weiss MH (2003) Pituitary anatomy and physiology. Neurosurg Clin N Am 14:11–23. https://doi.org/10.1016/s1042-3680(02)00017-7

Arafah BM (1986) Reversible hypopituitarism in patients with large nonfunctioning pituitary adenomas. J Clin Endocrinol Metab 62:1173–1179. https://doi.org/10.1210/jcem-62-6-1173

Arafah BM, Kailani SH, Nekl KE, Gold RS, Selman WR (1994) Immediate recovery of pituitary function after transsphenoidal resection of pituitary macroadenomas. J Clin Endocrinol Metab 79:348–354. https://doi.org/10.1210/jcem.79.2.8045946

Asa SL, Penz G, Kovacs K, Ezrin C (1982) Prolactin cells in the human pituitary—a quantitative immuno-cytochemical analysis. Arch Pathol Lab Med 106:360–363

Bargmann W (1949) The neurosecretory connection between the hypothalamus and the neurohypophysis. Z Zellforsch Mikrosk Anat 34:610–634

Bargmann W, Hild W, Ortmann R, Schiebler TH (1950) Morphologic and experimental studies of the hypothalamohypophyseal system. Acta Neuroveg (wien) 1:233–275

Bjarkam CR et al (2004) A MRI-compatible stereotaxic localizer box enables high-precision stereotaxic procedures in pigs. J Neurosci Methods 139:293–298. https://doi.org/10.1016/j.jneumeth.2004.05.004

Bjarkam CR, Glud AN, Orlowski D, Sorensen JC, Palomero-Gallagher N (2016) The telencephalon of the Gottingen minipig, cytoarchitecture and cortical surface anatomy. Brain Struct Funct. https://doi.org/10.1007/s00429-016-1327-5

Bjarkam CR, Glud AN, Orlowski D, Sorensen JCH, Palomero-Gallagher N (2017a) The telencephalon of the Gottingen minipig, cytoarchitecture and cortical surface anatomy. Brain Struct Funct 222:2093–2114. https://doi.org/10.1007/s00429-016-1327-5

Bjarkam CR, Orlowski D, Tvilling L, Bech J, Glud AN, Sørensen JCH (2017b) Exposure of the pig CNS for histological analysis: a manual for decapitation, skull opening and brain removal. J Vis Exp. https://doi.org/10.3791/55511

Bonthius DJ, McKim R, Koele L, Harb H, Karacay B, Mahoney J, Pantazis NJ (2004) Use of frozen sections to determine neuronal number in the murine hippocampus and neocortex using the optical disector and optical fractionator. Brain Res Brain Res Protoc 14:45–57. https://doi.org/10.1016/j.brainresprot.2004.09.003

Cao D, Ma X, Zhang WJ, Xie Z (2017) Dissection and coronal slice preparation of developing mouse pituitary gland. J vis Exp. https://doi.org/10.3791/56356

Catt KJ (1970) Pituitary function. Lancet 1:827–831. https://doi.org/10.1016/s0140-6736(70)92423-2

Christensen AB, Sorensen JCH, Ettrup KS, Orlowski D, Bjarkam CR (2018) Pirouetting pigs: a large non-primate animal model based on unilateral 6-hydroxydopamine lesioning of the nigrostriatal pathway. Brain Res Bull 139:167–173. https://doi.org/10.1016/j.brainresbull.2018.02.010

Console GM, Gomez Dumm CL, Brown OA, Ferese C, Goya RG (1997) Sexual dimorphism in the age changes of the pituitary lactotrophs in rats. Mech Ageing Dev 95:157–166. https://doi.org/10.1016/s0047-6374(97)01878-2

Console GM, Jurado SB, Oyhenart E, Ferese C, Pucciarelli H, Dumm CLAG (2001) Morphometric and ultrastructural analysis of different pituitary cell populations in undernourished monkeys. Braz J Med Biol Res 34:65–74. https://doi.org/10.1590/S0100-879x2001000100008

Cruz-Orive LM, Weibel ER (1990) Recent stereological methods for cell biology: a brief survey. Am J Physiol 258:L148-156

Cushing H (1912) The pituitary body and its disorders, clinical states produced by disorders of the hypophysis cerebri. vol x. J.B. Lippincott Company, Philadelphia

Dacheux F (1980) Ultrastructural immunocytochemical localization of prolactin and growth hormone in the porcine pituitary. Cell Tissue Res 207:277–286. https://doi.org/10.1007/BF00237812

Dacheux F (1981) Ultrastructural localization of corticotropin, beta-lipotropin, and alpha- and beta-endorphin in the porcine anterior pituitary. Cell Tissue Res 215:87–101. https://doi.org/10.1007/BF00236251

Dacheux F (1984) Differentiation of cells producing polypeptide hormones (ACTH, MSH, LPH, alpha- and beta-endorphin, GH and PRL) in the fetal porcine anterior pituitary. Cell Tissue Res 235:615–621. https://doi.org/10.1007/BF00226960

Dacheux F, Dubois MP (1976) Ultrastructural localization of prolactin, growth hormone and luteinizing hormone by immunocytochemical techniques in the bovine pituitary. Cell Tissue Res 174:245–260. https://doi.org/10.1007/BF00222162

Dada MO, Campbell GT, Blake CA (1984) Pars distalis cell quantification in normal adult male and female rats. J Endocrinol 101:87–94

de Lima AR et al (2007) Muscular dystrophy-related quantitative and chemical changes in adenohypophysis GH-cells in golden retrievers. Growth Horm IGF Res 17:480–491. https://doi.org/10.1016/j.ghir.2007.06.001

Deniz OG, Altun G, Kaplan AA, Yurt KK, von Bartheld CS, Kaplan S (2018) A concise review of optical, physical and isotropic fractionator techniques in neuroscience studies, including recent developments. J Neurosci Methods 310:45–53. https://doi.org/10.1016/j.jneumeth.2018.07.012

Ettrup KS et al (2011) Basic surgical techniques in the Gottingen minipig: intubation, bladder catheterization, femoral vessel catheterization, and transcardial perfusion. J vis Exp. https://doi.org/10.3791/2652

Filippa V, Mohamed F (2006b) Immunohistochemical study of somatotrophs in pituitary pars distalis of male viscacha (*Lagostomus maximus maximus*) in relation to the gonadal activity. Cells Tissues Organs 184:188–197. https://doi.org/10.1159/000099626

Filippa V, Mohamed F (2006a) ACTH cells of pituitary pars distalis of viscacha (*Lagostomus maximus maximus*): immunohistochemical study in relation to season, sex, and growth. Gen Comp Endocrinol 146:217–225. https://doi.org/10.1016/j.ygcen.2005.11.012

Filippa V, Mohamed F (2010) Morphological and morphometric changes of pituitary lactotrophs of viscacha (*Lagostomus maximus maximus*) in relation to reproductive cycle, age, and sex. Anat Rec (hoboken) 293:150–161. https://doi.org/10.1002/ar.21013

Francis SM, Venters SJ, Duxson MJ, Suttie JM (2000) Differences in pituitary cell number but not cell type between genetically lean and fat coopworth sheep. Domest Anim Endocrinol 18:229–239. https://doi.org/10.1016/s0739-7240(99)00081-8

Garcia-Navarro S, Malagon MM, Gracia-Navarro F (1988) Immunohistochemical localization of thyrotropic cells during amphibian morphogenesis: a stereological study. Gen Comp Endocrinol 71:116–123. https://doi.org/10.1016/0016-6480(88)90302-4

Glud AN et al (2011) Direct MRI-guided stereotaxic viral mediated gene transfer of alpha-synuclein in the Gottingen minipig CNS. Acta Neurobiol Exp (wars) 71:508–518

Glud AN, Bjarkam CR, Azimi N, Johe K, Sorensen JC, Cunningham M (2016) Feasibility of three-dimensional placement of human therapeutic stem cells using the intracerebral microinjection instrument. Neuromodul J Int Neuromodul Soc 19:708–716. https://doi.org/10.1111/ner.12484

Goodman S, Check E (2002) The great primate debate. Nature 417:684–687. https://doi.org/10.1038/417684a

Gundersen HJ (1986) Stereology of arbitrary particles. A review of unbiased number and size estimators and the presentation of some new ones, in memory of William R. Thompson. J Microsc 143:3–45

Gundersen HJ, Jensen EB (1987) The efficiency of systematic sampling in stereology and its prediction. J Microsc 147:229–263

Gundersen HJ et al (1988) The new stereological tools: disector, fractionator, nucleator and point sampled intercepts and their use in pathological research and diagnosis. APMIS 96:857–881

Harris GW (1948) Neural control of the pituitary gland. Physiol Rev 28:139–179. https://doi.org/10.1152/physrev.1948.28.2.139

Heidelbaugh JJ (2016) Endocrinology update: hypopituitarism. FP Essentials 451:25–30

Heiman J (1938) The anterior pituitary gland in tumor-bearing rats. Am J Cancer 33:423–442. https://doi.org/10.1158/ajc.1938.423

Heiman ML, Surface PL, Mowrey DH, DiMarchi RD (1990) Sexual dimorphic porcine pituitary response to growth hormone-releasing hormone. Domest Anim Endocrinol 7:273–276. https://doi.org/10.1016/0739-7240(90)90033-v

Hofmann I et al (2020) Linkage between growth retardation and pituitary cell morphology in a dystrophin-deficient pig model of Duchenne muscular dystrophy. Growth Horm IGF Res 51:6–16. https://doi.org/10.1016/j.ghir.2019.12.006

Hong GK, Payne SC, Jane JA Jr (2016) Anatomy, physiology, and laboratory evaluation of the pituitary gland. Otolaryngol Clin N Am 49:21–32. https://doi.org/10.1016/j.otc.2015.09.002

Jensen KN, Deding D, Sorensen JC, Bjarkam CR (2009) Long-term implantation of deep brain stimulation electrodes in the pontine micturition centre of the Gottingen minipig. Acta Neurochir 151:785–794. https://doi.org/10.1007/s00701-009-0334-1

Jurado S, Console G, Gomez Dumm C (1998) Sexually dimorphic effects of aging on rat somatotroph cells. An immunohistochemical and ultrastructural study. J Vet Med Sci 60:705–711. https://doi.org/10.1292/jvms.60.705

Kasper RS, Shved N, Takahashi A, Reinecke M, Eppler E (2006) A systematic immunohistochemical survey of the distribution patterns of GH, prolactin, somatolactin, beta-TSH, beta-FSH, beta-LH, ACTH, and Alpha-MSH in the Adenohypophysis of Oreochromis Niloticus, the Nile Tilapia. Cell Tissue Res 325:303–313. https://doi.org/10.1007/s00441-005-0119-7

Kiki I, Altunkaynak BZ, Altunkaynak ME, Vuraler O, Unal D, Kaplan S (2007) Effect of high fat diet on the volume of liver and quantitative feature of Kupffer cells in the female rat: a stereological and ultrastructural study. Obes Surg 17:1381–1388. https://doi.org/10.1007/s11695-007-9219-7

Koeppen BM, Stanton BA, Levy MN, Berne RM (2018) Berne & Levy physiology

Kovacs K, Horvath E, Asa SL, Stefaneanu L, Sano T (1989) Pituitary cells producing more than one hormone human pituitary adenomas. Trends Endocrinol Metab 1:104–107. https://doi.org/10.1016/1043-2760(89)90012-x

Kuwahara S, Sari DK, Tsukamoto Y, Tanaka S, Sasaki F (2004) Age-related changes in growth hormone (GH) cells in the pituitary gland of male mice are mediated by GH-releasing hormone but not by somatostatin in the hypothalamus. Brain Res 998:164–173. https://doi.org/10.1016/j.brainres.2003.10.060

Lee J-S (2006) Comparative study of immunocytochemical patterns of somatotrophs, mammotrophs, and mammosomatotrophs in the porcine anterior pituitary vol 1875. Digital Repository @ Iowa State University. http://lib.dr.iastate.edu/. https://doi.org/10.31274/rtd-180813-1876

Lee JS, Jeftinija K, Jeftinija S, Stromer MH, Scanes CG, Anderson LL (2004) Immunocytochemical distribution of somatotrophs in porcine anterior pituitary. Histochem Cell Biol 122:571–577. https://doi.org/10.1007/s00418-004-0715-8

Lillethorup TP et al (2018) Nigrostriatal proteasome inhibition impairs dopamine neurotransmission and motor function in minipigs. Exp Neurol 303:142–152. https://doi.org/10.1016/j.expneurol.2018.02.005

Lind NM, Moustgaard A, Jelsing J, Vajta G, Cumming P, Hansen AK (2007) The use of pigs in neuroscience: modeling brain disorders. Neurosci Biobehav Rev 31:728–751. https://doi.org/10.1016/j.neubiorev.2007.02.003

Mai JRK, Paxinos G (2012) The human nervous system, 3rd edn. Elsevier Academic Press, Amsterdam

Meijer JC, Trudeau VL, Colenbrander B, Poot P, Erkens JH, Van de Wiel DF (1988) Prolactin in the developing pig. Biol Reprod 39:264–269. https://doi.org/10.1095/biolreprod39.2.264

Mikami S, Chiba S, Hojo H, Taniguchi K, Kubokawa K, Ishii S (1988) Immunocytochemical studies on the pituitary pars distalis of the Japanese long-fingered bat, *Miniopterus schreibersii fuliginosus*. Cell Tissue Res 251:291–299

Milosevic V, Nestorovic N, Terzic M, Ristic N, Ajdzanovic V, Trifunovic S, Sekulic M (2009) Pituitary ACTH cells in female rats after neonatal treatment with SRIH-14. Folia Histochem Cytobiol 47:479–484. https://doi.org/10.2478/v10042-009-0104-1

Mitrofanova LB, Konovalov PV, Krylova JS, Polyakova VO, Kvetnoy IM (2017) Plurihormonal cells of normal anterior pituitary:

facts and conclusions. Oncotarget 8:29282–29299. https://doi.org/10.18632/oncotarget.16502
Molitch ME (2017) Diagnosis and treatment of pituitary adenomas: a review. JAMA 317:516–524. https://doi.org/10.1001/jama.2016.19699
Musumeci G et al (2015) A journey through the pituitary gland: development, structure and function, with emphasis on embryo-foetal and later development. Acta Histochem 117:355–366. https://doi.org/10.1016/j.acthis.2015.02.008
Naik DR, Shirasawa N, Nogami H, Ishikawa H (1991) Immunohistochemistry of the pituitary pars distalis of the musk shrew, *Suncus murinus*. Gen Comp Endocrinol 84:27–35
Nakane PK (1970) Classifications of anterior pituitary cell types with immunoenzyme histochemistry. J Histochem Cytochem 18:9–20. https://doi.org/10.1177/18.1.9
Nishimura S, Okano K, Yasukouchi K, Gotoh T, Tabata S, Iwamoto H (2000) Testis developments and puberty in the male Tokara (Japanese native) goat. Anim Reprod Sci 64:127–131. https://doi.org/10.1016/s0378-4320(00)00197-4
Norgaard Glud A et al (2010) Direct gene transfer in the Gottingen Minipig CNS Using stereotaxic lentiviral microinjections. Acta Neurobiol Exp (wars) 70:308–315
Orlowski D, Glud AN, Palomero-Gallagher N, Sorensen JCH, Bjarkam CR (2019) Online histological atlas of the Gottingen minipig brain. Heliyon 5:e01363. https://doi.org/10.1016/j.heliyon.2019.e01363
Orstrup LH et al (2019) Towards a Gottingen minipig model of adult onset growth hormone deficiency: evaluation of stereotactic electrocoagulation method. Heliyon 5:e02892. https://doi.org/10.1016/j.heliyon.2019.e02892
Ozone C et al (2016) Functional anterior pituitary generated in self-organizing culture of human embryonic stem cells. Nat Commun 7:10351. https://doi.org/10.1038/ncomms10351
Peter B, De Rijk EP, Zeltner A, Emmen HH (2016) Sexual maturation in the female Gottingen minipig. Toxicol Pathol 44:482–485. https://doi.org/10.1177/0192623315621413
Raus Balind S, Manojlovic-Stojanoski M, Milosevic V, Todorovic D, Nikolic L, Petkovic B (2016) Short- and long-term exposure to alternating magnetic field (50 Hz, 0.5 mT) affects rat pituitary ACTH cells: stereological study. Environ Toxicol 31:461–468. https://doi.org/10.1002/tox.22059
Rosendal F et al (2010) Defining the intercommissural plane and stereotactic coordinates for the Basal Ganglia in the Gottingen minipig brain. Stereotact Funct Neurosurg 88:138–146. https://doi.org/10.1159/000303526
Sasaki F, Iwama Y (1988) Sex difference in prolactin and growth hormone cells in mouse adenohypophysis: stereological, morphometric, and immunohistochemical studies by light and electron microscopy. Endocrinology 123:905–912. https://doi.org/10.1210/endo-123-2-905
Sauleau P, Lapouble E, Val-Laillet D, Malbert CH (2009) The pig model in brain imaging and neurosurgery. Anim. Int. J. Anim. Biosci. 3:1138–1151. https://doi.org/10.1017/S1751731109004649
Sterio DC (1984) The unbiased estimation of number and sizes of arbitrary particles using the disector. J Microsc 134:127–136
Tan JH, Sasaki F (2000) Effect of age on immunocytochemical staining characteristics of adenohypophyseal cells in *Mongolian pony mares* and stallions. Am J Vet Res 61:826–831. https://doi.org/10.2460/ajvr.2000.61.826
Trifunovic S, Manojlovic-Stojanoski M, Ajdzanovic V, Nestorovic N, Ristic N, Medigovic I, Milosevic V (2014) Effects of genistein on stereological and hormonal characteristics of the pituitary somatotrophs in rats. Endocrine 47:869–877. https://doi.org/10.1007/s12020-014-0265-3
Trifunovic S et al (2016) Effects of prolonged alcohol exposure on somatotrophs and corticotrophs in adult rats: stereological and hormonal study. Acta Histochem 118:353–360. https://doi.org/10.1016/j.acthis.2016.03.005
Trifunovic S, Manojlovic-Stojanoski M, Nestorovic N, Ristic N, Sosic-Jurjevic B, Pendovski L, Milosevic V (2018) Histological and morphofunctional parameters of the hypothalamic–pituitary–adrenal system are sensitive to daidzein treatment in the adult rat. Acta Histochem 120:129–135. https://doi.org/10.1016/j.acthis.2017.12.006
Trouillas J, Guigard MP, Fonlupt P, Souchier C, Girod C (1996) Mapping of corticotropic cells in the normal human pituitary. J Histochem Cytochem 44:473–479. https://doi.org/10.1177/44.5.8627004
Vanputten LJA, Vanzwieten MJ, Mattheij JAM, Vankemenade JAM (1988) Studies on prolactin-secreting cells in aging rats of different strains. 1 Alterations in pituitary histology and serum prolactin levels as related to aging. Mech Ageing Dev 42:75–90. https://doi.org/10.1016/0047-6374(88)90064-4
Vidal S, Roman A, Moya L (1997) Description of two types of mammosomatotropes in mink (*Mustela vison*) adenohypophysis: changes in the population of mammosomatotropes under different physiological conditions. Acta Anat (basel) 159:209–217. https://doi.org/10.1159/000147986
Wang JF et al (2014) Establishment and characterization of dairy cow growth hormone secreting anterior pituitary cell model. In Vitro Cell Dev Biol Anim 50:103–110. https://doi.org/10.1007/s11626-013-9664-7
Watanabe H, Andersen F, Simonsen CZ, Evans SM, Gjedde A, Cumming P, DaNe XSG (2001) MR-based statistical atlas of the Gottingen minipig brain. Neuroimage 14:1089–1096. https://doi.org/10.1006/nimg.2001.0910
West MJ (2012) Basic stereology for biologists and neuroscientists. Cold Spring Harbor Laboratory Press
West MJ (2013) Tissue shrinkage and stereological studies. Cold Spring Harb Protoc. https://doi.org/10.1101/pdb.top071860
West MJ, Slomianka L, Gundersen HJ (1991) Unbiased stereological estimation of the total number of neurons in thesubdivisions of the rat hippocampus using the optical fractionator. Anat Rec 231:482–497. https://doi.org/10.1002/ar.1092310411
Willems C, Fu Q, Roose H, Mertens F, Cox B, Chen J, Vankelecom H (2016) Regeneration in the pituitary after cell-ablation injury: time-related aspects and molecular analysis. Endocrinology 157:705–721. https://doi.org/10.1210/en.2015-1741
Wolpert SM, Molitch ME, Goldman JA, Wood JB (1984) Size, shape, and appearance of the normal female pituitary gland. AJR Am J Roentgenol 143:377–381. https://doi.org/10.2214/ajr.143.2.377